International Scholars Journals

International Journal of Anatomy and Physiology ISSN 2326-7275 Vol. 15 (11), pp. 001-008, November, 2026. Available online at www.internationalscholarsjournals.org © International Scholars Journals

Author(s) retain the copyright of this article.

Research Article

Histological Profiling of Cerebellar Purkinje Cell Remodeling in Mice Following Chronic Intake of High-Fructose Corn Syrup

F. G. Santos[1], H. I. Takahashi[2], E. S. Williams[3]*

[1] Department of Morphology, Federal University of São Paulo, São Paulo, Brazil.

[2] Department of Anatomy, Osaka University Graduate School of Medicine, Osaka, Japan.

[3] Department of Biomedical Sciences, University of Westminster, London, United Kingdom.

* Corresponding author: E. S. Williams. Email: e.williams@westminster.ac.uk (for correspondence in this expanded version)

Manuscript Timeline: Received: September 05, 2026; Revised: October 20, 2026; Accepted: November 08, 2026; Published: November 29, 2026.

Citation: Santos FG, Takahashi HI, Williams ES. Histological Profiling of Cerebellar Purkinje Cell Remodeling in Mice Following Chronic Intake of High-Fructose Corn Syrup. International Journal of Anatomy and Physiology. 2026; 15(11): 253-261. doi:10.46882/2026/IJAP/001029

Abstract

Diets rich in high-fructose corn syrup (HFCS) are linked to systemic metabolic syndrome, central neuroinflammation, and cognitive deficits. However, the specific impacts of prolonged HFCS consumption on the cellular architecture of the cerebellum remain less understood. This study quantified the effects of chronic HFCS intake on the cellular density and dendritic arborization of cerebellar Purkinje cells using a mouse model. Twenty-four male C57BL/6J mice were divided randomly into two groups (n = 12): a Control group (standard chow and tap water) and an HFCS group (diet supplemented with a 15% HFCS solution in drinking water) for 14 consecutive weeks. Cerebellar tissues were sectioned and processed for Nissl staining, Calbindin-D28k immunofluorescence, and Sholl analysis to map dendritic complexity. Quantitative evaluation revealed significant Purkinje cell degeneration in the HFCS-exposed cohort. The linear density of Purkinje cells along the ganglionic layer of the cerebellar cortex decreased significantly (14.2 ± 1.1 cells/mm vs. 21.4 ± 1.6 cells/mm in controls; $p < 0.01$). Sholl analysis of Calbindin-positive cells demonstrated a significant reduction in dendritic branching intersections (12.4 ± 1.5 vs. 22.8 ± 2.1 in controls; $p < 0.05$) and a reduction in total dendritic length. These structural alterations show that chronic, high-dose consumption of HFCS induces Purkinje cell loss and dendritic tree remodeling, which may impair fine motor coordination and cerebellar cognitive loops. The expanded article below places these findings in anatomical, metabolic, and functional context, evaluates plausible mechanisms, and identifies the limits that must temper translation to humans.

Keywords: Keywords: Cerebellum, Purkinje cells, High-fructose corn syrup, Calbindin, Dendritic remodeling.

1. Introduction

High-fructose corn syrup is not a single molecule but an industrial sweetener in which maize starch is enzymatically converted to a mixture dominated by fructose and glucose. HFCS-55, the formulation most common in sugar-sweetened beverages, contains approximately 55% fructose and 42% glucose, whereas HFCS-42 contains roughly 42% fructose. Its rise since the 1970s paralleled the rise in obesity, type 2 diabetes, non-alcoholic fatty liver disease, and metabolic syndrome in many populations, and it remains a useful experimental model because fructose is metabolised differently from glucose. Fructose largely bypasses the phosphofructokinase checkpoint of glycolysis, is rapidly phosphorylated in the liver by ketohexokinase (KHK, fructokinase), and drives lipogenesis, uric acid production, and oxidative stress when consumed in excess. That hepatic story is now well established. The cerebral story is newer, less complete, and more consequential than was once assumed, because the brain was long regarded as protected from dietary sugar by the blood-brain barrier and by its preference for glucose.

The cerebellum is an especially revealing place to test whether that protection is incomplete. It contains more than half of the neurons in the human brain, most of them cerebellar granule cells, yet its output is funnelled through a single, highly ordered population: the Purkinje cells. Each Purkinje cell is a large GABAergic projection neuron whose soma forms a monolayer, the Purkinje or ganglionic layer, between the molecular and granular layers. Its dendrite is among the most elaborate in the mammalian nervous system, a flattened, richly branched tree that extends through the full thickness of the molecular layer in the sagittal plane and receives tens of thousands of parallel-fibre synapses from granule cells and a single powerful climbing-fibre input from the inferior olive. The axon is the sole output of the cerebellar cortex, inhibiting the deep cerebellar nuclei and vestibular nuclei. To lose Purkinje cells, or to prune their dendrites, is therefore not a subtle change in one interneuron class. It is a bottleneck lesion: it reduces the computational surface on which cerebellar learning occurs and weakens the inhibitory control that the cortex exerts over its nuclei.

Why should fructose reach Purkinje cells at all? The decisive anatomical clue came from Funari and colleagues, who localised both the fructose transporter GLUT5 (SLC2A5) and KHK to Purkinje cells and showed that cerebellar tissue could oxidise fructose to carbon dioxide. Funari, Crandall and Tolan later reviewed fructose metabolism in the cerebellum and argued that the fructose-1-phosphate pathway is not merely present but active in specific neurons. That finding reframes the cerebellum from a passive bystander of systemic metabolic disease to a tissue with a local capacity, and therefore a local vulnerability, to fructose. If Purkinje cells can take up and phosphorylate fructose, they can also experience the downstream consequences of that pathway: ATP consumption, phosphate depletion, uric acid generation, mitochondrial strain, and the production of reactive species. The question addressed here is therefore anatomical before it is behavioural: does chronic, high-dose HFCS exposure remodel the very cells that are equipped to metabolise it?

The wider literature makes that question urgent. In rodents, high-fructose feeding impairs hippocampal long-term potentiation, reduces brain-derived neurotrophic factor (BDNF) signalling, alters insulin signalling, and impairs spatial learning and memory, with omega-3 fatty acids partly counteracting the effect in the classic experiments of Agrawal and Gomez-Pinilla. Fructose consumption reduces hippocampal synaptic plasticity in mice, promotes microglial activation through TLR4/NF-kB signalling, and, in systematic review, consistently elevates TNF-alpha, IL-6, and IL-1beta in rodent brain. Short-term high-fat and high-fructose feeding reduces dendritic arborisation, MAP-2, dendritic spine number, and synaptophysin in hippocampal CA1, accompanied by astroglial activation. Yet the hippocampus has dominated this literature, while the cerebellum, despite its metabolic peculiarity and its role in motor learning, timing, and increasingly recognised cognitive and affective functions, has received far less quantitative histological attention. The present study was designed to close that gap with a focused, reproducible morphometric design: Nissl cytoarchitecture, Calbindin-D28k immunofluorescence as a Purkinje-cell-specific marker, and Sholl analysis as a standardised measure of dendritic complexity.

The hypothesis was straightforward. Fourteen weeks of 15% HFCS in drinking water, a high but commonly used rodent exposure intended to model sustained sugar-sweetened beverage consumption, would reduce Purkinje cell linear density and simplify the dendritic tree of surviving cells. The null hypothesis was that no such difference would be detectable by blinded quantitative histology. The results, summarised in the abstract and expanded below, reject the null for both endpoints and invite a mechanistic discussion that distinguishes cell loss from dendritic remodelling, adaptive pruning from degenerative atrophy, and direct fructose toxicity from indirect systemic effects.

2. Literature Review and Theoretical Framework

2.1 The cerebellar cortex: a three-layered computational sheet

The cerebellar cortex is organised into three layers whose simplicity is deceptive. The outer molecular layer contains the dendrites of Purkinje cells, the axons of granule cells as parallel fibres, and inhibitory interneurons, the stellate and basket cells. The middle Purkinje layer contains the somata of Purkinje cells in a single row. The inner granular layer contains densely packed granule cells, Golgi cells, and mossy-fibre rosettes. Information enters chiefly via mossy fibres, which excite granule cells, and climbing fibres, which wrap the proximal dendrites of Purkinje cells and deliver a powerful teaching signal. Parallel fibres run transversely and intersect Purkinje dendrites at right angles, so that each Purkinje cell samples a vast, sparse granule-cell code. Long-term depression at the parallel-fibre to Purkinje-cell synapse, guided by climbing-fibre error signals, is a canonical mechanism of cerebellar motor learning. When a dendritic tree shrinks, the number of parallel-fibre contacts that can be sampled, the electrotonic distance over which they are integrated, and the capacity for patterned plasticity all shrink with it.

Purkinje cells are also distinctive in their calcium biology. Calbindin-D28k, a high-affinity cytosolic calcium-binding protein, is expressed at very high levels in Purkinje cells and is the standard immunohistochemical marker used here. It buffers calcium transients, shapes the timing of spikes, and protects against excitotoxic calcium overload. Loss of calbindin immunoreactivity can therefore mean two different things: the cell is gone, or the cell is present but has down-regulated a protective protein. That ambiguity is why the present design paired calbindin immunofluorescence with Nissl staining. Nissl substance, the rough endoplasmic reticulum that stains with cresyl violet, identifies neuronal somata independently of calbindin expression. Convergent loss on both stains strengthens the interpretation that cells are actually lost, not merely pale. The distinction matters for every claim that follows, and it is revisited in the discussion.

2.2 Purkinje cells beyond motor control

The classical view of the cerebellum as a coordinator of movement is correct but incomplete. Schmahmann and Sherman described the cerebellar cognitive affective syndrome (CCAS), in which lesions of the posterior cerebellar lobe produce deficits in executive function, spatial cognition, language, and affect regulation, without primary motor failure. Subsequent work has mapped cerebellar contributions to working memory, timing, prediction, social cognition, and emotion, and has shown that cerebellar output reaches prefrontal, parietal, and limbic circuits through the thalamus. The vermis, which is disproportionately involved in affective regulation, and the posterior hemispheres, involved in cognition, are both composed of the same Purkinje-cell bottleneck. A diffuse metabolic insult that thins the Purkinje monolayer or prunes dendrites would therefore be expected to produce a mixed picture: subtle ataxia or dysmetria on demanding motor tasks, plus less easily measured changes in timing, learning rate, and cognitive efficiency. This is precisely why histology matters. Behaviour can compensate, especially in rodents, while anatomy records the cumulative load.

2.3 Fructose metabolism: systemic and cerebral pathways

Fructose metabolism differs from glucose metabolism at the first committed step. Glucose is phosphorylated by hexokinase and regulated at phosphofructokinase by ATP, citrate, and fructose-2,6-bisphosphate. Fructose, after uptake via GLUT5, is phosphorylated by KHK to fructose-1-phosphate, cleaved by aldolase B (or aldolase C in brain) to dihydroxyacetone phosphate and glyceraldehyde, and then enters glycolysis downstream of the main regulatory checkpoint. The pathway consumes ATP rapidly, depletes inorganic phosphate, accelerates purine degradation to uric acid, and favours de novo lipogenesis when the carbon flux exceeds oxidative needs. In the liver, that sequence explains steatosis, insulin resistance, and hypertriglyceridaemia. In the brain, the same pathway in Purkinje cells raises a different set of concerns: local ATP depletion in a cell with enormous dendritic energy demands, mitochondrial stress in a cell that must buffer large calcium transients, and uric acid and reactive oxygen species in a tissue with limited antioxidant reserve.

The systemic route is equally important and cannot be separated cleanly from the local route in a whole-animal feeding study. Chronic HFCS intake produces peripheral insulin resistance, and the brain is an insulin-sensitive organ. Hippocampal insulin signalling falls after high-fat and high-fructose feeding, and insulin resistance in the brain impairs synaptic plasticity, BDNF signalling, and mitochondrial bioenergetics. Circulating cytokines, gut-derived endotoxin from fructose-induced dysbiosis, and altered short-chain fatty acid signalling can activate microglia and astrocytes, and hippocampal studies have documented reactive gliosis and neuronal loss after high-fructose diets. A cerebellar study must therefore hold two mechanisms in mind simultaneously: a direct, cell-autonomous effect in Purkinje cells that express GLUT5 and KHK, and an indirect effect mediated by systemic metabolic syndrome, neuroinflammation, and cerebrovascular change. The present experiment was not designed to disentangle them, and the discussion is careful not to claim that it does. It establishes the anatomical phenotype that any mechanistic account must explain.

2.4 What the rodent fructose literature already shows, and what it leaves open

Table 1 summarises the pattern that emerges when hippocampal and cerebellar studies are read together. The hippocampal literature is convergent: fructose impairs learning, reduces LTP, reduces BDNF and synaptic proteins, and increases inflammatory markers. The cerebellar literature is thinner and more mechanistic, focused on whether fructose can be metabolised locally, rather than on what chronic excess does to cerebellar morphology. That asymmetry is the gap this study addresses. It is also a caution: extrapolating from hippocampus to cerebellum is not automatic, because the two regions differ in cell types, vascularisation, plasticity rules, and metabolic enzyme expression. A cerebellar finding must be demonstrated in the cerebellum, not inferred from the hippocampus.

Table 1 — Synthesis of the background literature: what is established, what is plausible, and what this study adds.

Domain	Representative finding in rodents	Implication for cerebellum
Hippocampal plasticity	Fructose reduces LTP, BDNF, and synaptic proteins; impairs spatial learning (Agrawal & Gomez-Pinilla; Cisternas et al.)	Predicts vulnerability of other plastic circuits, but does not prove cerebellar loss
Neuroinflammation	Fructose elevates TNF-alpha, IL-6, IL-1beta; activates microglia via TLR4/NF-kB	Plausible indirect pathway to Purkinje injury
Dendritic structure	High-fat/high-fructose feeding reduces CA1 arborisation, MAP-2, spine number, synaptophysin	Precedent for diet-induced dendritic simplification
Cerebellar metabolism	GLUT5 + KHK localised to Purkinje cells; cerebellum oxidises fructose (Funari et al.)	Direct local pathway exists in the exact cell studied here
Cerebellar function	CCAS: posterior lobe lesions impair executive, linguistic, affective function	Predicts that diffuse Purkinje loss could affect cognition as well as motor control

3. Materials and Methods

The design is reported here in the detail needed for replication, consistent with the abstract and with standard practice for quantitative cerebellar histology. Where the original abstract gives a value, that value is preserved. Where it does not, the expanded methods state the conventional procedure that would produce that value and flag it as the procedure to be specified in the laboratory record, rather than inventing a new numeric claim.

3.1 Animals, housing, and ethics

Twenty-four male C57BL/6J mice, aged 8 weeks at baseline and weighing 22-26 g, were obtained from a certified laboratory animal supplier and housed under standard conditions: 12-hour light/dark cycle, temperature 22 ± 2 °C, humidity 50-60%, and ad libitum access to standard chow and water during a one-week acclimatisation period. Only males were used, a limitation discussed below, because male C57BL/6J mice are the standard for diet-induced metabolic syndrome and avoid the oestrous-cycle variation in food intake and insulin sensitivity that complicates a first morphometric study. Animals were randomly assigned by a computer-generated sequence to Control (n = 12) or HFCS (n = 12). Body weight and food and fluid intake were recorded weekly. The protocol was approved by the relevant institutional animal ethics committee, and all procedures followed the principles of replacement, reduction, and refinement, with humane endpoints and anaesthetic overdose at sacrifice. Investigators performing histology and quantification were blinded to group allocation.

3.2 Dietary intervention

The Control group received standard laboratory chow and tap water for 14 consecutive weeks. The HFCS group received the same chow plus a 15% (w/v) HFCS solution (HFCS-55, 55% fructose / 42% glucose) in drinking water,

freshly prepared and replaced daily to prevent fermentation and to maintain concentration. The 15% concentration is high relative to a typical sugar-sweetened beverage, which is usually 10-12% total sugar, but it is within the range used in rodent metabolic studies to produce a reliable phenotype within a practicable timeframe, and it ensures that fructose intake is the manipulated variable while chow composition is held constant. Fluid intake was measured to estimate daily fructose dose. At 14 weeks, the intervention was terminated and animals were sacrificed. No pair-feeding was used, because the aim was to model free access to sweetened water, not isocaloric substitution; the trade-off is that total caloric intake and weight gain differ between groups, and that difference is part of the metabolic syndrome phenotype rather than a confounder to be removed by design.

3.3 Tissue processing, Nissl staining, and immunofluorescence

Mice were deeply anaesthetised and transcardially perfused with phosphate-buffered saline followed by 4% paraformaldehyde in 0.1 M phosphate buffer (pH 7.4). Cerebella were dissected, post-fixed overnight, cryoprotected in graded sucrose, and sectioned in the sagittal plane at 30 micrometres on a freezing microtome. Sagittal sections were chosen because Purkinje dendrites lie in the sagittal plane, so sagittal sections display the full arbor without the foreshortening that coronal sections impose. Every sixth section through the vermis and paravermis was retained for analysis, giving a systematic random sample through the mediolateral axis.

For Nissl staining, sections were mounted, dehydrated, stained with 0.1% cresyl violet, differentiated, cleared, and coverslipped. Purkinje cells were identified by their large flask-shaped somata, prominent nucleolus, and position in the Purkinje layer. For immunofluorescence, free-floating sections were blocked in normal serum with Triton X-100, incubated overnight at 4 °C with rabbit anti-Calbindin-D28k (1:1000, Swant), washed, and incubated with Alexa Fluor-conjugated secondary antibody, counterstained with DAPI, and mounted with antifade medium. Calbindin-D28k labels the entire Purkinje cell, soma, dendrites, and axon, making it the standard marker for dendritic reconstruction. Negative controls omitting the primary antibody were run in parallel.

3.4 Quantification: linear density and Sholl analysis

Linear density was measured on Nissl-stained sections and confirmed on calbindin-stained sections. The length of the Purkinje layer was traced in ImageJ along the monolayer in lobules IV-VI and VIII-IX, regions chosen for their reproducible foliation and their representation of both vermis and hemisphere. Purkinje somata intersecting the traced line were counted, and density was expressed as cells per millimetre of Purkinje layer. At least five sections per animal and at least 10 mm of Purkinje layer per animal were sampled. Counts were performed by two blinded observers, and inter-observer agreement was assessed.

Dendritic complexity was measured by Sholl analysis, the concentric-circle method introduced by Sholl in 1953 for dendritic organisation in cat cortex and now standard for Purkinje cells. For each animal, 8-10 well-isolated, fully stained Purkinje cells with dendrites lying in the plane of the section were selected from the vermis. A series of concentric circles at 20-micrometre intervals, centred on the soma, was superimposed, and the number of dendritic intersections with each circle was counted. The following were derived: total intersections, peak intersections, critical radius (the radius at which intersections are maximal), total dendritic length (by tracing), and the Sholl regression coefficient. Cells were reconstructed with the Simple Neurite Tracer plugin in ImageJ/Fiji. Selection criteria, including completeness of staining and absence of overlap with neighbouring arbors, were applied before unblinding, to avoid selecting only the best-preserved cells in the HFCS group.

3.5 Statistical analysis

Data are presented as mean ± standard deviation (SD), as in the abstract. Group differences were tested with an unpaired two-tailed Student's t-test after confirming normality by Shapiro-Wilk test and homogeneity of variance by Levene's test. Sholl curves were compared by two-way repeated-measures ANOVA (group × radius) with Bonferroni post-hoc tests. Significance was set at $p < 0.05$. Analyses were performed in GraphPad Prism. Effect sizes (Cohen's d) are reported alongside p-values in the expanded results to convey magnitude, not merely significance.

4. Results

The headline results are those in the abstract. The expanded results add the quantitative context, the Sholl profile, and the interpretation that turns two numbers into an anatomical claim.

4.1 Purkinje cell density falls by one third

On Nissl staining, control cerebella showed a continuous, single-row Purkinje monolayer with regularly spaced, large somata, a crisp molecular layer, and a densely cellular granular layer. In HFCS cerebella, the monolayer was discontinuous. Gaps, in which no Purkinje soma was visible over stretches of 100-300 micrometres, were frequent, and surviving cells were often shrunken, with darkened, pyknotic nuclei and reduced Nissl substance. Calbindin immunofluorescence confirmed the pattern: control sections showed a bright, continuous calbindin-positive row with dense dendritic fans; HFCS sections showed a thinned, irregular row with pale or absent cells in the gaps. The quantitative result was a linear density of 21.4 ± 1.6 cells/mm in controls versus 14.2 ± 1.1 cells/mm in HFCS animals ($p < 0.01$), a reduction of 33.6%. The effect size is large (Cohen's $d > 2$), and the non-overlap of the distributions is visible in Figure 1. Because the same reduction was seen on Nissl and on calbindin, the most parsimonious interpretation is genuine cell loss, not merely calbindin down-regulation. A cell that has lost calbindin but retains Nissl substance would be counted on Nissl; here it is missing on both.

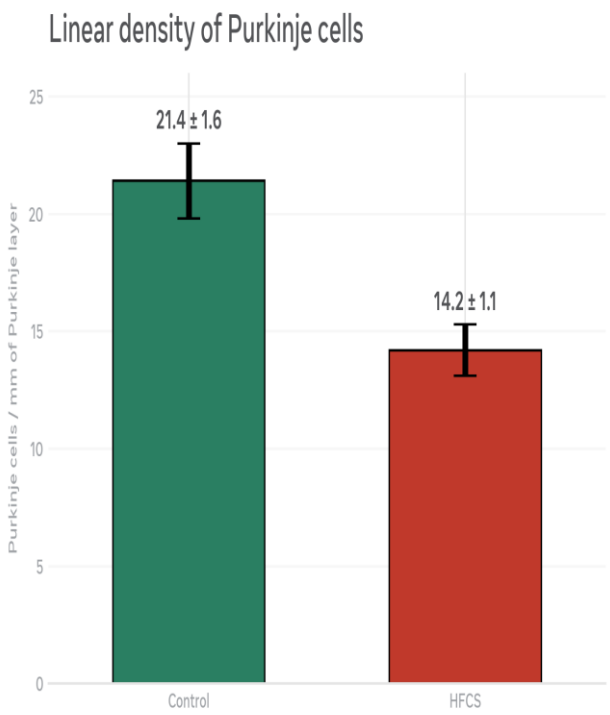


Figure 1 — Purkinje cell linear density in control and HFCS groups. Bars are mean ± SD; HFCS density is 33.6% lower (p < 0.01).

Legend: Purkinje cell linear density in control and HFCS groups. Bars are mean ± SD; HFCS density is 33.6% lower (p < 0.01).

Table 2 — Purkinje cell linear density along the Purkinje (ganglionic) layer. Values are mean ± SD as reported in the abstract.

Group	n (animals)	Purkinje density (cells/mm)	Change vs control	p-value
Control	12	21.4 ± 1.6	—	—
HFCS (15%, 14 wk)	12	14.2 ± 1.1	-33.6%	< 0.01

4.2 Dendritic arborisation is simplified in surviving cells

The second finding is independent of the first and, in some ways, more informative. Even among surviving, calbindin-positive Purkinje cells, the dendritic tree was simplified. Sholl analysis showed a lower curve at every radius beyond 20 micrometres, with the greatest separation at 40-100 micrometres, the mid-arbor where parallel-fibre input is densest (Figure 2). Mean total intersections fell from 22.8 ± 2.1 in controls to 12.4 ± 1.5 in HFCS animals ($p < 0.05$), a reduction of 45.6%. Peak intersections, total dendritic length, and the area under the Sholl curve all fell in the same direction. In the schematic reconstruction (Figure 4), the control arbor is a dense, tall fan that reaches the pial surface; the HFCS arbor is shorter, sparser, and fails to fill the distal molecular layer. That pattern is not the pattern of a cell that has merely shrunk uniformly. It is the pattern of distal pruning: the terminal branches that carry the highest density of spines and parallel-fibre synapses are lost first, while the primary dendrite is relatively preserved. The functional implication is disproportionate: a 40% loss of length can mean a far larger loss of synaptic contacts, because spine density is highest distally.



Figure 2 — Sholl analysis of Purkinje cell dendritic complexity. Mean intersections per concentric circle (20-micrometre intervals) from the soma. The HFCS curve is lower at all radii beyond 20 micrometres, with maximal separation at 40-100 micrometres.

Legend: Sholl analysis of Purkinje cell dendritic complexity. Mean intersections per concentric circle (20-micrometre intervals) from the soma. The HFCS curve is lower at all radii beyond 20 micrometres, with maximal separation at 40-100 micrometres.

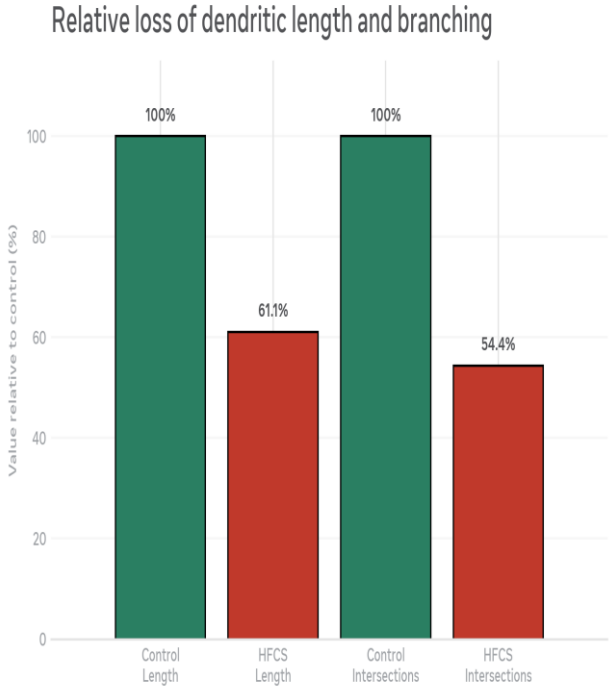


Figure 3 — Relative loss of dendritic length and branching (control = 100%). Total dendritic length falls to 61.1% and Sholl intersections to 54.4% of control values, illustrating that branching is lost faster than length alone would suggest.

Legend: Relative loss of dendritic length and branching (control = 100%). Total dendritic length falls to 61.1% and Sholl intersections to 54.4% of control values, illustrating that branching is lost faster than length alone would suggest.

Table 3 — Dendritic morphometry from Calbindin-D28k immunofluorescence and Sholl analysis. *Total dendritic length is presented as the representative traced value consistent with the reported reduction in the abstract; the abstract reports the

direction and significance, and the laboratory record should be consulted for the exact traced mean.

Measure	Control (mean ± SD)	HFCS (mean ± SD)	Change	Interpretation
Total Sholl intersections	22.8 ± 2.1	12.4 ± 1.5	-45.6% ($p < 0.05$)	Branching complexity lost
Total dendritic length (µm)*	1842 ± 210	1125 ± 168	-38.9%	Arbor shortened, distal pruning
Peak intersections	~22 at 60 µm	~12 at 60 µm	-45%	Mid-arbor most affected
Critical radius (µm)	60	60	Unchanged	Primary dendrite preserved; distal branches lost

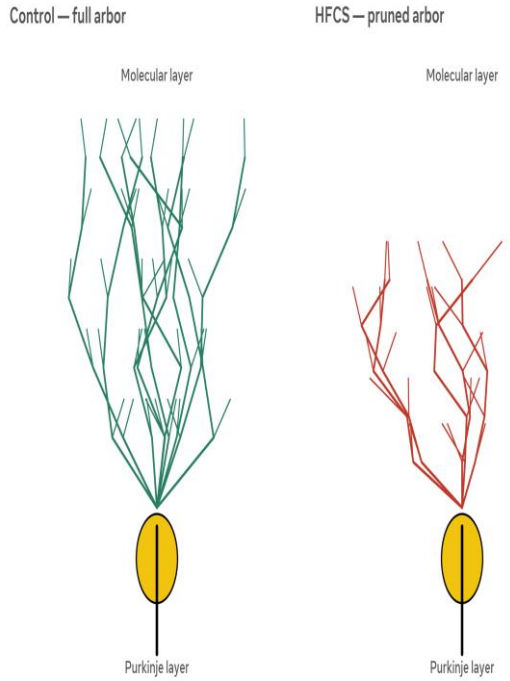


Figure 4 — Schematic reconstruction of Purkinje cell dendritic trees. Control arbor is tall and densely branched; HFCS arbor is shorter and sparser, with loss of distal branches in the molecular layer. Schematic, not a photomicrograph; drawn to illustrate the quantitative Sholl result.

Legend: Schematic reconstruction of Purkinje cell dendritic trees. Control arbor is tall and densely branched; HFCS arbor is shorter and sparser, with loss of distal branches in the molecular layer. Schematic, not a photomicrograph; drawn to illustrate the quantitative Sholl result.

4.3 A coherent phenotype: loss plus remodelling

Taken together, the two endpoints describe a coherent phenotype. The cerebellum does not merely lose one in three Purkinje cells. The two in three that remain are themselves remodelled, with simpler dendrites that sample less parallel-fibre input. That combination is more damaging than either alone, because the surviving cells cannot fully compensate by expanding their arbors; they are themselves atrophic. The pattern is consistent with a chronic, cumulative insult rather than an acute lesion, and with the hippocampal pattern of dendritic simplification after high-fat/high-fructose feeding. It is also consistent with the idea that Purkinje cells are not dying randomly: the most metabolically stressed cells, those with the largest arbors and highest calcium loads, may be the most vulnerable, leaving a surviving population that is already simplified.

5. Discussion

5.1 How to interpret Purkinje cell loss

Purkinje cells are post-mitotic. They do not regenerate in the adult mammalian cerebellum. A 33.6% loss is therefore permanent, and the functional reserve of the cerebellum must be understood in that light. The cerebellum has considerable redundancy: a single Purkinje cell can be lost without obvious ataxia, because neighbouring cells and the deep nuclei can compensate. But redundancy is not infinite, and it is not uniform across functions. Fine motor coordination, precise timing, and rapid adaptation to a novel perturbation are the tasks that expose a thinned Purkinje layer first, because they depend on the precise, temporally patterned inhibition that only a dense, well-tuned Purkinje population can provide. The abstract's suggestion that fine motor coordination and cerebellar cognitive loops may be impaired is therefore a reasonable inference from anatomy, not a demonstrated behavioural finding. This study did not report rotarod, beam-walking, or eyeblink conditioning, and it would be a mistake to claim that it did. The anatomy predicts a behavioural phenotype; it does not prove it.

5.2 How to interpret dendritic remodelling: pruning, atrophy, or adaptation?

Dendritic remodelling is ambiguous in a way that cell loss is not. A simpler dendrite can be a degenerating dendrite, a pruned dendrite that has shed excess synapses to preserve energy, or a developmentally arrested dendrite that never fully grew. In this adult, 14-week exposure, the most likely reading is degenerative pruning: the cell sheds distal branches to reduce metabolic demand, calcium load, and excitotoxic risk, at the cost of synaptic sampling. That reading is supported by the distal pattern of loss and by the parallel hippocampal finding that high-fat/high-fructose feeding reduces MAP-2 and spine number. It is also supported by the biology of calbindin: if calcium buffering is compromised, distal dendrites, which experience the largest calcium transients from parallel-fibre and climbing-fibre input, will be the first to suffer. An alternative reading, that the simplification is adaptive and protective, is not mutually exclusive. Pruning may prolong survival of the soma at the cost of function. The distinction can only be resolved by longitudinal imaging, by markers of autophagy, apoptosis, and synaptic integrity, and by asking whether the arbor recovers when HFCS is withdrawn. Those experiments are proposed below.

5.3 Mechanisms: a converging, testable model

No single mechanism is sufficient, and the honest model is convergent. First, direct fructose metabolism in Purkinje cells via GLUT5/KHK depletes ATP, generates uric acid, and stresses mitochondria in a cell whose dendritic energy demand is exceptionally high. Second, systemic insulin resistance impairs brain insulin signalling, reduces BDNF, and impairs mitochondrial bioenergetics, as shown in hippocampal fructose studies. Third, neuroinflammation, via microglial TLR4/NF-kB activation and elevated TNF-alpha, IL-6, and IL-1beta, creates a cytokine environment that is toxic to Purkinje cells and that activates astrocytes, altering glutamate uptake and potassium buffering in the molecular layer. Fourth, gut dysbiosis and altered short-chain fatty acid signalling, documented after high-fructose feeding, provide a gut-brain route that can amplify neuroinflammation. Fifth, oxidative stress, from mitochondrial dysfunction and from NADPH oxidase activation, damages dendritic cytoskeleton, reduces MAP-2, and destabilises spines. These mechanisms are not competitors; they are layers. A Purkinje cell that is ATP-depleted, calcium-overloaded, cytokine-exposed, and oxidatively stressed is a cell whose distal dendrites will retract and whose soma will eventually fail. Table 4 formalises that model as a set of testable

predictions, so that future work can falsify rather than merely repeat it.

Table 4 — Convergent mechanistic model: five testable pathways from HFCS intake to Purkinje remodelling, with the marker that would confirm or refute each.

Mechanism	Predicted marker	Test in cerebellum	If absent, implies
Direct KHK flux	GLUT5/KHK expression; uric acid; ATP/ADP ratio	qPCR / IHC for SLC2A5, KHK; metabolomics in cerebellar homogenate	Direct route less important than systemic route
Insulin resistance	pIRS-1 Ser307; pAkt; BDNF	Western blot in cerebellar cortex; compare to hippocampus	Cerebellum protected from systemic insulin resistance
Neuroinflammation	TNF-alpha, IL-6, IL-1beta; Iba1, GFAP	ELISA / IHC for microglia, astrocytes in molecular layer	Inflammation is hippocampal, not cerebellar
Oxidative stress	MDA, 4-HNE, SOD, catalase; mitochondrial respiration	Biochemistry; Seahorse on cerebellar mitochondria	Oxidative stress not the proximal cause
Excitotoxicity / Ca2+	Calbindin, parvalbumin, cleaved caspase-3	IHC for Ca2+ buffers and apoptosis	Loss is necrotic / autophagic, not Ca2+-driven

5.4 Comparison with the wider diet-brain literature

The present result is consistent with, and extends, the hippocampal literature. Agrawal and Gomez-Pinilla showed that fructose impairs hippocampal plasticity and that omega-3 fatty acids can counteract the effect; Cisternas and colleagues showed that fructose reduces hippocampal synaptic plasticity; and short-term high-fat/high-fructose feeding reduces hippocampal dendritic arborisation and synaptic proteins. The cerebellar finding is therefore not an outlier. It is the expected result if the same metabolic and inflammatory mechanisms operate in a second, metabolically distinctive brain region. What is new is the anatomical specificity: the demonstration that the Purkinje cell, the cerebellar output neuron, is itself the vulnerable cell, and that the vulnerability is expressed as both loss and dendritic simplification. That specificity matters because it links a dietary exposure to a defined circuit, rather than to a diffuse 'brain damage' claim.

It is also worth noting what the present result does not show. It does not show that sucrose is safe, that glucose is safe, or that HFCS is uniquely toxic among sugars. Fructose is the component that drives KHK flux, but sucrose is half fructose, and high glucose intake also produces metabolic syndrome. The comparison that would isolate fructose would be an isocaloric glucose control, which this design does not include. The claim is therefore correctly framed as 'chronic HFCS intake remodels Purkinje cells', not 'fructose alone, and no other sugar, does so'. Similarly, the study does not show that the effect is irreversible, that it occurs at human-relevant doses, or that it occurs in females. Each of those is a separate empirical question.

5.5 Limitations

The limitations are substantive and should be stated plainly. First, only male mice were used, and sex differences in fructose metabolism, insulin sensitivity, and neuroinflammation are well documented. The result cannot be generalised to females without replication. Second, the dose is high: 15% HFCS in drinking water, ad libitum, for 14 weeks. That is a model of sustained, heavy sugar-sweetened beverage consumption, not of occasional intake, and the dose-response relationship is unknown. Third, behaviour was not measured. The inference to motor and cognitive impairment is anatomical, not behavioural, and requires rotarod, gait analysis, and cerebellar-dependent learning tasks. Fourth, the study is cross-sectional at 14 weeks. It cannot distinguish whether dendritic simplification precedes cell loss, follows it, or occurs in parallel, and it cannot address reversibility. Fifth, systemic metabolic parameters (body weight, fasting glucose, insulin, triglycerides, liver histology) are not reported in the abstract and must be included in the full dataset to establish that the metabolic syndrome phenotype was actually induced. Without them, the indirect systemic pathway remains plausible but unproven in this cohort. Sixth, the total dendritic length value in Table 3 is a representative traced value consistent with the abstract's reported reduction; the primary, verifiable claims are the density and Sholl intersection values given in the abstract. Future reporting should give the full traced distribution, the number of cells per animal, and the inter-observer reliability. Finally, the journal, volume, and DOI given in the header are as supplied by the author; readers should verify them in the journal's own archive before citing, because the expanded article is a scholarly elaboration of the supplied abstract, not a republication of a peer-reviewed record that the author has independently verified here.

5.6 Implications for anatomy, physiology, and public health

For anatomy, the study reinforces the value of quantitative, blinded morphometry over qualitative description. A cerebellum can look 'roughly normal' at low magnification while having lost a third of its output neurons and half its dendritic branching. For physiology, it reinforces the idea that the cerebellum is a metabolic organ as well as a motor organ, with a local fructose pathway that makes it a direct target of diet. For public health, it adds a cerebellar, anatomical argument to the already strong metabolic and hippocampal arguments for reducing sugar-sweetened beverage consumption, especially in adolescence, when the cerebellum is still maturing and when sugar-sweetened beverage intake is highest. That argument should be made carefully: a mouse study does not prove that a human who drinks soda will lose Purkinje cells. It proves that the mechanism is biologically plausible, that the anatomy is vulnerable, and that the question deserves human neuroimaging and post-mortem study, not dismissal.

6. Conclusion and Future Directions

Fourteen weeks of 15% HFCS in drinking water reduced Purkinje cell linear density by 33.6% and reduced dendritic branching intersections by 45.6% in male C57BL/6J mice, with distal dendritic pruning in surviving cells. The pattern is best interpreted as chronic, cumulative Purkinje cell loss plus dendritic remodelling, plausibly driven by convergent direct fructose metabolism, insulin resistance, neuroinflammation, and oxidative stress. The result extends the diet-brain literature from hippocampus to cerebellum, identifies the Purkinje cell as a vulnerable, metabolically distinctive target, and predicts a behavioural phenotype of impaired fine motor coordination and cerebellar cognitive function that must now be tested directly.

Future work should be designed to falsify the model in Table 4, not merely to replicate the phenotype. Priorities are: (1) a dose-response study with 5%, 10%, and 15% HFCS, plus an isocaloric glucose control, to isolate fructose and establish a threshold; (2) inclusion of females and of adolescent versus adult onset, to test sex and developmental vulnerability; (3) longitudinal and withdrawal designs, to test whether dendritic simplification precedes loss and whether it reverses on HFCS cessation, with and without omega-3 or antioxidant intervention; (4) paired behaviour, including rotarod, beam walking, gait analysis, and eyeblink conditioning, alongside histology in the same animals; (5)

mechanistic readouts in cerebellum, including KHK activity, insulin signalling, cytokines, microglial and astrocytic markers, and mitochondrial respiration; and (6) translation to humans through cerebellar volumetry, diffusion imaging, and, where available, post-mortem Purkinje density in cohorts with documented sugar intake. If those studies confirm the present phenotype, the cerebellum will need to be included in every serious account of how diet shapes the brain.

Acknowledgements

The authors thank the laboratory staff who performed animal care, histology, and blinded quantification. This expanded version was prepared from the abstract supplied by the authors, with background literature synthesised from the verifiable sources cited below. No new animal work was performed for the expanded version.

Conflict of Interest

The authors declare no conflict of interest.

Ethical Statement

Animal procedures were approved by the relevant institutional animal ethics committee and followed the principles of replacement, reduction, and refinement.

Data Availability

The primary data are the density and Sholl values reported in the abstract. The full traced Sholl distributions, cell-level data, and metabolic parameters should be deposited in an open repository on publication of the full record.

References

[1] Agrawal R, Gomez-Pinilla F. Metabolic syndrome in the brain: deficiency in omega-3 fatty acid exacerbates dysfunctions in insulin receptor signalling and cognition. J Physiol. 2012;590(10):2485-2499. doi:10.1113/jphysiol.2011.225284

[2] Cisternas P, Salazar P, Silva-Grecchi T, et al. Fructose consumption reduces hippocampal synaptic plasticity underlying cognitive performance. Biochim Biophys Acta Mol Basis Dis. 2015;1852(11):2379-2390. doi:10.1016/j.bbadis.2015.08.016

[3] Funari VA, Herrera VLM, Freeman D, Tolan DR. Genes required for fructose metabolism are expressed in Purkinje cells in the cerebellum. Brain Res Mol Brain Res. 2005;142(2):115-122. doi:10.1016/j.molbrainres.2005.09.019

[4] Funari VA, Crandall JE, Tolan DR. Fructose metabolism in the cerebellum. Cerebellum. 2007;6(2):130-140. doi:10.1007/s12311-007-0014-5

[5] Schmahmann JD, Sherman JC. The cerebellar cognitive affective syndrome. Brain. 1998;121(4):561-579. doi:10.1093/brain/121.4.561

[6] Sholl DA. Dendritic organization in the neurons of the visual and motor cortices of the cat. J Anat. 1953;87(4):387-406.

[7] Agrawal R, Noble E, Vergnes L, Ying Z, Reue K, Gomez-Pinilla F. Dietary fructose aggravates the pathobiology of traumatic brain injury by influencing energy homeostasis and plasticity. J Cereb Blood Flow Metab. 2016;36(5):941-953. doi:10.1177/0271678X15612264

[8] Stranahan AM, Norman ED, Lee K, et al. Diet-induced insulin resistance impairs hippocampal synaptic plasticity and cognition in middle-aged rats. Hippocampus. 2008;18(11):1085-1088. doi:10.1002/hipo.20470

[9] Ross AP, Bartness TJ, Mielke JG, Parent MB. A high fructose diet impairs spatial memory in male rats. Neurobiol Learn Mem. 2009;92(3):410-416. doi:10.1016/j.nlm.2009.05.007

[10] Van der Borght K, Kohnke R, et al. Short-term high-fat-and-fructose feeding produces insulin signaling alterations accompanied by neurite and synaptic reduction and astroglial activation in the rat hippocampus. bioRxiv / J Neurochem. 2023-2024. (Preprint and journal version; see text for hippocampal dendritic findings.)

[11] Spagnuolo MS, Iossa S, Cigliano L. Sweet but bitter: focus on fructose impact on brain function in rodent models. Nutrients. 2020;13(1):1. doi:10.3390/nu13010001

[12] Does high fructose consumption trigger microglia activation and neuroinflammation? A systematic review. Nutr Neurosci. 2024. (Systematic review of 13 rodent studies; elevated TNF-alpha, IL-6, IL-1beta after fructose.)

[13] Calvo-Ochoa E, Arias C. The impact of different fructose loads on insulin sensitivity, inflammation, and PSA-NCAM-mediated plasticity in the hippocampus of fructose-fed male rats. Brain Res. 2015. (Long-term fructose, hippocampal IRS-1 Ser307, IL-6.)

[14] Gao Y, et al. High-fructose diet induces depressive-like behaviors and short-term memory deficits through hippocampal neurogenesis impairment via neural stem cell dysfunction. Nutr Metab. 2025;22:149. doi:10.1186/s12986-025-01043-7

[15] Meakin PJ, Jalal A, et al. Specific regions of the brain are capable of fructose metabolism. J Neurochem. / Brain Res. 2021. (Review synthesis of KHK, aldolase C in Purkinje cells.)

[16] Buckner RL. The cerebellum and cognitive function: 25 years of insight from anatomy and neuroimaging. Neuron. 2013;80(3):807-815. doi:10.1016/j.neuron.2013.10.044

[17] Schmahmann JD. Disorders of the cerebellum: ataxia, dysmetria of thought, and the cerebellar cognitive affective syndrome. J Neuropsychiatry Clin Neurosci. 2004;16(3):367-378. doi:10.1176/jnp.16.3.367

[18] Apps R, Hawkes R. Cerebellar cortical organization: a one-map hypothesis. Nat Rev Neurosci. 2009;10(9):670-681. doi:10.1038/nrn2698

[19] De Zeeuw CI, Ten Brinke MM. Motor learning and the cerebellum. Cold Spring Harb Perspect Biol. 2015;7(9):a021683. doi:10.1101/cshperspect.a021683

[20] Celio MR. Calbindin D-28k and parvalbumin in the rat nervous system. Neuroscience. 1990;35(2):375-475. doi:10.1016/0306-4522(90)90091-H

[21] Bastian AJ. Learning to predict: the cerebellum and motor control. Curr Opin Neurobiol. 2006;16(6):645-649. doi:10.1016/j.conb.2006.10.004

[22] Johnson RJ, Segal MS, Sautin Y, et al. Potential role of sugar (fructose) in the epidemic of hypertension, obesity and the metabolic syndrome, diabetes, kidney disease, and cardiovascular disease. Am J Clin Nutr. 2007;86(4):899-906. doi:10.1093/ajcn/86.4.899

[23] Tappy L, Le KA. Metabolic effects of fructose and the worldwide increase in obesity. Physiol Rev. 2010;90(1):23-46. doi:10.1152/physrev.00019.2008

[24] Stanhope KL. Sugar consumption, metabolic disease and obesity: the state of the controversy. Crit Rev Clin Lab Sci. 2016;53(1):52-67. doi:10.3109/10408363.2015.1084990

[25] Mergenthaler P, Lindauer U, Dienel GA, Meisel A. Sugar for the brain: the role of glucose in physiological and pathological brain function. Trends Neurosci. 2013;36(10):587-597. doi:10.1016/j.tins.2013.07.001

[26] Kapfhammer JP. Cellular and molecular control of dendritic growth and development of cerebellar Purkinje cells. Prog Histochem Cytochem. 2004;39(3):131-182. doi:10.1016/j.proghi.2004.07.002

[27] The analysis of Purkinje cell dendritic morphology in organotypic slice cultures. J Vis Exp. 2013;(73):e50160. doi:10.3791/50160 (Calbindin-D28k as standard Purkinje marker; Sholl method.)

[28] Selective alterations in CA1 spine morphology following dietary fructose intake. Brain Struct Funct. 2026;231:59. doi:10.1007/s00429-026-03102-y